Largest Lyapunov exponent in molecular systems. II: Quaternion coordinates and application to methane clusters

F. Calvo*

Laboratoire Collisions, Agrégats, Réactivité, CNRS UMR 5589, Institut de Recherche sur les Systèmes Atomiques et Moléculaires Complexes, Université Paul Sabatier, 118 Route de Narbonne, F31062 Toulouse Cedex, France

(Received 15 January 1999)

We present a numerical procedure for extracting Lyapunov characteristic exponents from classical molecular-dynamics simulations of molecular systems. The theoretical frame chosen to describe the orientational degrees of freedom is the quaternions scheme. We apply the method to small methane clusters. Two different model potentials are used to investigate the role of internal molecular motion on the nonlinear dynamics, and several parameters are calculated to study the thermodynamics and chaotic dynamics of these clusters. Evidence is found for a solidlike to plasticlike phase transition occurring with the release of the orientational degrees of freedom, at low temperatures below the melting point. The largest Lyapunov exponent increases significantly during this transition, but it exhibits no particular variation during melting. [S1063-651X(99)14108-4]

PACS number(s): 05.45.Pq, 05.70.Fh, 36.40.−c

I. INTRODUCTION

The relationship between the microscopic time dynamics of a complex system and its macroscopic behavior may be investigated in several ways. The standard tools of statistical physics, for instance in the field of liquids theory [1], can be efficiently used to predict various quantities experimentally measurable at bulk level. With the increasing interest in nonlinear physics, other fundamental questions have been addressed more directly, such as the paradox of macroscopic irreversibility [2–4] established by Loschmidt in 1876. Indeed, one of the most intriguing features of many-body atomic systems, even bound by simple potentials such as Lennard-Jones (LJ), is that they are chaotic. In other words, and despite the time reversibility of the equations of motion, the dynamics is unstable in the sense of Lyapunov: two trajectories which are initially close to each other in the phase space exponentially diverge in time. Up to now, this fact has been mainly supported by numerical experiments [5,6], but also more recently by analytical models [7]. However, since complex atomic systems are far from being integrable, there is no doubt that chaos is a widely spread phenomenon in these species.

Some useful parameters to quantify chaos are the Lyapunov characteristic exponents. They are defined as the exponential rates of local divergence or convergence of trajectories in the phase space. In the case of ''simple'' chaotic systems with only few degrees of freedom (DOF), the largest Lyapunov exponent λ has been seen to be generally a good indicator of the possible crises [8], even though not systematically [9]. Several works have shown that, in the case of atomic systems, the largest Lyapunov exponent λ could be used as an indicator of a phase change. This seems to be true at least for large systems near the thermodynamic limit [3,10], but is not as simple for clusters having only a few DOF. In the case of realistic molecular systems, evidence from previous works [11–14] indicates that the internal orientational DOF play a part at least as important as that of the translational DOF in the short-time dynamics. In their studies on water, Ohmine and co-workers [12,13] have developed the instantaneous normal mode (INM) approach of Buchner *et al.* [14] to three-dimensional molecular systems. The basic idea here is to look at the full anharmonicities exhibited by the forces and torques between molecules, in order to separate the respective contributions of all the collective modes to the dynamics.

As molecular systems display a much greater diversity of phases than simple atomic systems, there is a real interest in studying dynamical parameters such as the Lyapunov exponents. From the thermodynamical point of view, the orientational DOF can be released before the translational DOF. The corresponding ''plastic'' phase transition can even be seen at finite size [15]. In particular, it may be responsible, as in the case of molecular nitrogen [11], for the main increase in the largest Lyapunov exponent, while only smooth variations are seen during the release of the translational DOF, that is, at melting. The Lyapunov exponents, in their finite-time local form, can also contribute to detect nonergodicity from the different probability distributions exhibited by different initial conditions [16]. This is important in simulation, as common atomic or molecular systems often exhibit problems of ''broken ergodicity'' or ''nonergodicity,'' even for small clusters such as LJ_7 [17].

Recent advances in methodology have led in the past years to the computation of Lyapunov characteristic exponents in hard-core [18] or molecular [11,19,20] systems. Diatomic molecular fluids have been investigated specifically [19,20] and, in a previous paper [11], we have proposed a method for estimating Lyapunov exponents in simulations of general molecular systems made of linear molecules. Now we extend this method to the case of three-dimensional molecules. We have chosen the quaternion frame of Evans [21]

*Present address: Département de Recherche Fondamentale sur la Matière Condensée, CEA Grenoble, 17 rue des Martyrs, F38054 Grenoble Cedex, France. Electronic address: fcalvo@cea.fr

to describe the internal coordinates, as it is probably the most robust and widely used scheme in numerical experiments on many rigid-body molecules. The next section recalls the main equations of motion, and presents the general method. In Sec. III we illustrate it with two examples of small methane clusters with 3 and 13 molecules, respectively. Finally, we briefly summarize and conclude in Sec. IV.

II. METHODOLOGY

We consider a molecular system of n molecules interacting through a potential-energy function V. Each molecule i with mass m_i contains n_i atoms or pseudoatoms, and is treated as a rigid body. In the principal axes of inertia, the inertia tensor $\mathbf{J}_i$ is diagonal with values J_i^x, J_i^y, and J_i^z. The translational motion is described with the center-of-mass coordinate $\mathbf{r}_i$ and the associated linear momentum $\mathbf{p}_i = m_i \dot{\mathbf{r}}_i$. The orientational motion is described with the quaternion $\mathbf{q}_i$ and the angular momentum $\boldsymbol{\pi}_i$ in the space-fixed reference frame. The main practical interest of the quaternion coordinates is that they remove the difficulties found when using Euler angles (θ, φ, ψ), namely that divergences occur in the rotational equations of motion when $\sin\theta \to 0$ [22,23]. Physically, they can be seen as the generalization to three-dimensional molecules of the orientation vector $\mathbf{e}$ for linear molecules. A good discussion on this subject is given by Goldstein [22]. Knowing the quaternion $\mathbf{q}_i = (q_0, q_1, q_2, q_3)$, one can calculate the instantaneous rotation matrix $\mathbf{Q}_i$ leading from molecular-fixed to space-fixed coordinates [23]:

$$\mathbf{Q}_i(\mathbf{q}_i) = \begin{pmatrix} q_0^2+q_1^2-q_2^2-q_3^2 & 2(q_1q_2+q_0q_3) & 2(q_1q_3-q_0q_2) \\ 2(q_1q_2-q_0q_3) & q_0^2-q_1^2+q_2^2-q_3^2 & 2(q_2q_3+q_0q_1) \\ 2(q_1q_3+q_0q_2) & 2(q_2q_3-q_0q_1) & q_0^2-q_1^2-q_2^2+q_3^2 \end{pmatrix}. \tag{1}$$

Denoting by $\mathbf{f}_i(\{\mathbf{r}_j, \mathbf{q}_j\})$ and $\boldsymbol{\tau}_i(\{\mathbf{r}_j, \mathbf{q}_j\})$ the respective total force and torque felt by molecule i, one can write the instantaneous equations of motion for both the translational and orientational part as [23]:

$$\frac{d\mathbf{r}_i}{dt} = \frac{1}{m_i}\mathbf{p}_i, \tag{2}$$

$$\frac{d\mathbf{p}_i}{dt} = \mathbf{f}_i(\{\mathbf{r}_j, \mathbf{q}_j\}), \tag{3}$$

$$\frac{d\boldsymbol{\pi}_i}{dt} = \boldsymbol{\tau}_i(\{\mathbf{r}_j, \mathbf{q}_j\}), \tag{4}$$

$$\frac{d\mathbf{q}_i}{dt} = \frac{1}{2}\mathcal{M}(\mathbf{q}_i)\begin{pmatrix} 0 \\ \boldsymbol{\omega}_i^b \end{pmatrix}. \tag{5}$$

In Eq. (5), $\mathcal{M}(\mathbf{q}_i)$ is the following 4×4 matrix:

$$\mathcal{M}(\mathbf{q}_i) = \begin{pmatrix} q_0 & -q_1 & -q_2 & -q_3 \\ q_1 & q_0 & -q_3 & q_2 \\ q_2 & q_3 & q_0 & -q_1 \\ q_3 & -q_2 & q_1 & q_0 \end{pmatrix} \tag{6}$$

and $\boldsymbol{\omega}_i^b$ is the body-fixed angular velocity vector in the principal molecular axes: $\boldsymbol{\omega}_i^b = \mathbf{J}_i^{-1}\mathbf{Q}_i(\mathbf{q}_i)\boldsymbol{\pi}_i$. At each time, these equations ensure the conservation of the quaternion norm, $|\mathbf{q}_i|^2 = q_0^2+q_1^2+q_2^2+q_3^2 = 1$. Numerically, they can be efficiently solved for a large variety of force types using accurate predictor-corrector algorithms [23], or more simply second-order Verlet-like algorithms [24].

In order to calculate Lyapunov exponents from such molecular-dynamics (MD) simulations, we write Eqs. (2)–(5) in concise form as

$$\frac{d\psi}{dt} = F(\psi), \tag{7}$$

where $\psi = \{\mathbf{r}_i, \mathbf{q}_i, \mathbf{p}_i, \boldsymbol{\pi}_i\}$ is a $13n$-vector and F a nonlinear function. Suppose now that ψ varies by an infinitesimal amount $\delta\psi(0)$ at time $t=0$. The subsequent time evolution of $\delta\psi$ leads to the largest Lyapunov exponent λ_1, provided that a metric $\|\ \|$ is defined on the phase space with dimension $13n$:

$$\lambda_1 = \lim_{t\to\infty} \lim_{\|\delta\psi(0)\|\to 0} \frac{1}{t} \ln \frac{\|\delta\psi(t)\|}{\|\delta\psi(0)\|}. \tag{8}$$

Differentiating Eqs. (2)–(5) is the natural way for obtaining the dynamical equations governing the variations of $\delta\psi$. It can be easily seen that

$$\frac{d\,\delta\psi}{dt} = \frac{\partial F}{\partial \psi}\delta\psi = \begin{pmatrix} \mathbf{0} & \mathbf{0} & \mathbf{A} & \mathbf{0} \\ \mathbf{0} & \mathbf{B} & \mathbf{0} & \mathbf{C} \\ \mathbf{D} & \mathbf{E} & \mathbf{0} & \mathbf{0} \\ \mathbf{F} & \mathbf{G} & \mathbf{0} & \mathbf{0} \end{pmatrix}\delta\psi, \tag{9}$$

where $\mathbf{A}$, $\mathbf{D}$, $\mathbf{E}$, $\mathbf{F}$, $\mathbf{G}$ are $3n\times3n$ matrices, $\mathbf{B}$ is a $4n\times4n$ matrix, and $\mathbf{C}$ is a $4n\times3n$ matrix forming the Jacobian $\partial F/\partial\psi$ along with the null matrices $\mathbf{0}$. All these matrices explicitly depend on the instantaneous phase-space vector ψ. In practice, it is not necessary to develop the full expressions for $\mathbf{A}, \ldots, \mathbf{G}$ to compute the Lyapunov characteristic exponents, and we show in the Appendix how an efficient implementation can be used in MD simulations.

As one follows a microcanonical molecular-dynamics trajectory for the vector $\psi(t)$, the largest Lyapunov exponent λ is calculated with Eq. (9) by the usual method first described by Benettin *et al.* [25]. This method involves calculating the variations of the vector $\delta\psi(t)$, assuming an initial value ε

for $\|\delta\psi(0)\|$, and recording periodically the length $\|\delta\psi(t)\|$. Due to the exponential divergence of $\delta\psi$, one also needs to rescale it. Other exponents can be estimated in the same way, by following a set of orthogonal vectors $\delta\psi_k$ and recording their lengths $\|\delta\psi_k(t)\|$ regularly. To maintain orthogonality, and to prevent the collapse of all vectors in the most rapidly growing direction, an orthonormalization procedure should be applied each time the lengths are calculated. Of course, the choice of the initial vectors $\delta\psi_k(0)$, as well as the check during orthonormalization, must incorporate the quaternion normalization $\delta|\mathbf{q}_i|^2=0$. Thus, the full spectrum of $13n$ exponents can be calculated from Eq. (9). It is also possible to compute the rotation numbers ω_k which quantify the average angular velocity of the vectors $\delta\psi_k$ in phase space. These parameters may be very useful in the study of dynamical systems, even if they have been only rarely considered up to now [4,19,26]. Another way of calculating the k largest Lyapunov exponents is to introduce $k(k-1)/2$ Lagrange multipliers on the right-hand side of Eq. (9) in order to constrain orthogonality of the set of k vectors in phase space [27]. It seems, however, that periodic reorthonormalization is still required due to numerical errors.

III. APPLICATION TO SMALL METHANE CLUSTERS

Due to their small number of degrees of freedom, atomic clusters are ideal test cases for numerical experiments on chaos in realistic systems. In fact, many previous simulations have focused on Lennard-Jones or Morse clusters [28] as prototype chaotic Hamiltonian models. Berry, Wales, and co-workers [29] have performed a detailed analysis of the relationship between the local characteristics of the potential-energy surface (PES) and the Lyapunov instability in small clusters. Their main conclusion is that negative curvature on the PES is the principal source of chaos in these systems. In large systems and in the bulk, the fluctuations of positive curvature seem to play an important part in the value of the Lyapunov exponents [30]. While the largest exponent strongly increases at the onset of melting in periodic systems [10], the situation appears more complicated in atomic clusters. Depending on the potential chosen to model the interaction between atoms, the variations of λ with total energy are very different [6,31]. In the case of nitrogen molecular clusters [11], the maximal Lyapunov exponent (MLE) can be used as a probe of the phase change occurring with the release of the internal degrees of freedom, even at small sizes. In the case of LJ clusters [31], there seems to be only a small increase in the MLE for clusters that are large enough (containing at least 38 atoms), but this increase is still continuous due to dynamical coexistence.

To illustrate the method presented in the preceding section, we have chosen to study the variations of the MLE λ with internal energy E in classical isoenergetic molecular-dynamics simulations of small $(CH_4)_n$ clusters. The choice of methane was made for several reasons. Contrary to other molecular van der Waals clusters experimentally studied such as $(SF_6)_n$ [32], methane clusters display very isotropic intermolecular forces, leading to a high crystalline crossover size [15] above which the structure is fcc. This similarity with simple atomic van der Waals clusters such as argon is responsible for the existence of very different kinds of model potentials for methane.

These potentials can be divided into two major categories: the united-atom (UA) models and the all-atom (AA) models. While the former ones treat the whole CH_4 molecule as a single pseudoatom, thus allowing much extensive simulations, the AA models are more appropriate for simulations in condensed phases. Therefore, it is possible to investigate with these model potentials the direct influence of the internal degrees of freedom on the chaotic behavior of methane clusters. Another motivation is to study the real microscopic dynamics and the statistical thermodynamics in detail, in contrast to most investigations on alkane clusters, which have been more concerned with large systems such as liquid droplets [33].

We have chosen a simple 12–6 Lennard-Jones UA model with parameters taken from Ref. [34], $\varepsilon=148.1$ K and $\sigma=3.73$ Å , to represent the interaction between CH_4 molecules. Among the various AA models, we have chosen one which gives satisfactory results on bulk simulations [35], namely the OPLS model [36]. This model uses 12–6 LJ interactions between all atoms of different molecules, as well as Coulombic interactions to model the octupole. The CH_4 molecule has a perfect tetrahedral geometry, with C–H distance being 1.09 Å . The LJ parameters are, respectively, $\varepsilon_{CC}=33.2$ K, $\varepsilon_{HH}=15.1$ K, $\sigma_{CC}=3.50$ Å , and $\sigma_{HH}=2.50$ Å . The parameters ε_{CH} and σ_{CH} are found with the usual Lorentz-Berthelot combination rules: $\varepsilon_{CH}=\sqrt{\varepsilon_{CC}\varepsilon_{HH}}$, $\sigma_{CH}=(\sigma_{CC}+\sigma_{HH})/2$. Finally, each carbon atom carries a charge of $+0.24e$, and each hydrogen atom a charge of $-0.06e$.

The two cluster sizes studied, with $n=3$ and $n=13$ molecules, respectively, were first investigated statically. We searched for the equilibrium geometries using the Monte Carlo basin-hopping method of Wales and Doye [37]. The translational and orientational displacements were performed alternatively, with a probability $p=0.1$ of performing a translational move. This is similar, in a way, to the molecular version of the basin-hopping algorithm developed recently by Wales and Hodges [38]. Our result is an equilateral triangle for the centers of mass of the CH_4 molecules in the $(CH_4)_3$ cluster, and an icosahedron in the case of $(CH_4)_{13}$. No particular order was found for the molecular orientations.

The calculation of the largest Lyapunov exponent requires integrating Eq. (9) along a MD trajectory. This is done in practice with a fourth-order Runge-Kutta scheme. For the main trajectory, such an algorithm is not necessary, and the leap-frog method of Fincham adapted to quaternions [24] is used. This algorithm has a moderate numerical cost and it naturally incorporates the quaternion normalization. During the simulations, we recorded several quantities of physical interest, besides the MLE. First, as we have already done for linear molecules [11], we evaluate a translational exponent λ_T by propagating a $6n$-vector $\delta\psi_T(t)$ according to the following equation:

$$\frac{d\,\delta\psi_T}{dt}=\begin{pmatrix}\mathbf{0} & \mathbf{A}\\ \mathbf{D} & \mathbf{0}\end{pmatrix}\delta\psi_T, \tag{10}$$

where the $3n\times 3n$ matrices $\mathbf{A}$ and $\mathbf{D}$ are those in Eq. (9). Let

us also emphasize that λ_T is *not* a real Lyapunov exponent, as it is not strictly associated to a complete set of equations of a dynamical system. However, all the important properties of the Lyapunov exponents (Oseledec's theorems) should still be valid for λ_T. To check for the possibility of isomerization phenomena, we calculated the root mean square of the bond length fluctuation, also known as the Lindemann parameter δ. The orientational disorder in methane clusters was analyzed using a generalization of the Vieillard-Baron parameter θ [23] to three-dimensional molecules:

$$\theta = \frac{1}{3} \sum_{j,k} \langle \mathbf{Q} \rangle^{jk}, \tag{11}$$

where $\langle \mathbf{Q} \rangle^{jk}$ is the (j,k) component of the matrix $\langle \mathbf{Q} \rangle$ defined from the molecular rotation matrices $\mathbf{Q}_i(t)$ as the average:

$$\langle \mathbf{Q} \rangle = \lim_{T \to \infty} \frac{1}{T} \int_0^T \frac{1}{n} \sum_{i=1}^{n} [\mathbf{Q}_i^{\dagger}(t) \mathbf{Q}_i(0)] dt \tag{12}$$

($\mathbf{Q}_i^{\dagger}$ is the transpose of $\mathbf{Q}_i$). Obviously, and in order that θ be significant, the simulations had to be performed with zero angular momentum. As in the case of linear molecules, θ has the value 0 in a perfectly disordered phase and the value 1 in a perfectly orientationally ordered state. An advantage of the definition (11) for θ is that it is independent of the molecular geometry. Other molecular species such as SF_6 can be further investigated with other tools [39,40], in particular projection methods such as the Pawley-Fuchs projection [41]. To prevent evaporation or fragmentation, which are likely to occur at high energies, we also added a repulsive potential wall: $V_{\rm rep}(r_i) = \kappa [r_i - R]^4/4$, where r_i is the distance of the molecular center of mass of molecule i with respect to the cluster center of mass, and R is the radius of the wall. $V_{\rm rep}$ is calculated only for distances r_i greater than R. The numerical parameters are $\kappa = 10^4$ K/Å^2, $R = 7.5$ Å for $(CH_4)_3$, and $R = 12.0$ Å for $(CH_4)_{13}$. Finally, we calculated the thermodynamical characteristic functions using the distributions of potential energies accumulated along the MD trajectories, and the multiple histogram method [42]. From simulations, we thus computed the (canonical) internal energy $U(T)$ and heat capacity $C(T) = \partial U / \partial T$.

All simulations were carried out with a time step of 5 fs for a total length of 7.5 ns at each energy. The first 2.5 ns were retained to allow thermalization, and the calculation of all quantities (averages, Lyapunov exponent) was initiated. Only the last 2.5 ns were kept for determining the average value of λ, while the last 5 ns were kept for δ, θ, and the histograms of potential energies.

We have represented in Fig. 1 the variations with internal energy E of the translational (δ) and orientational (θ) order parameters for the clusters $(CH_4)_3$ and $(CH_4)_{13}$. We have also plotted the Lindemann index determined using the UA model. The configurational heat capacities are plotted in Fig. 2 versus the canonical temperature T for both the UA and AA models. From the thermodynamical point of view, the clusters undergo a phase change from solidlike to liquidlike at approximately 40–50 K in the case of the AA model, and in the vicinity of 30–40 K for the UA model. This phase

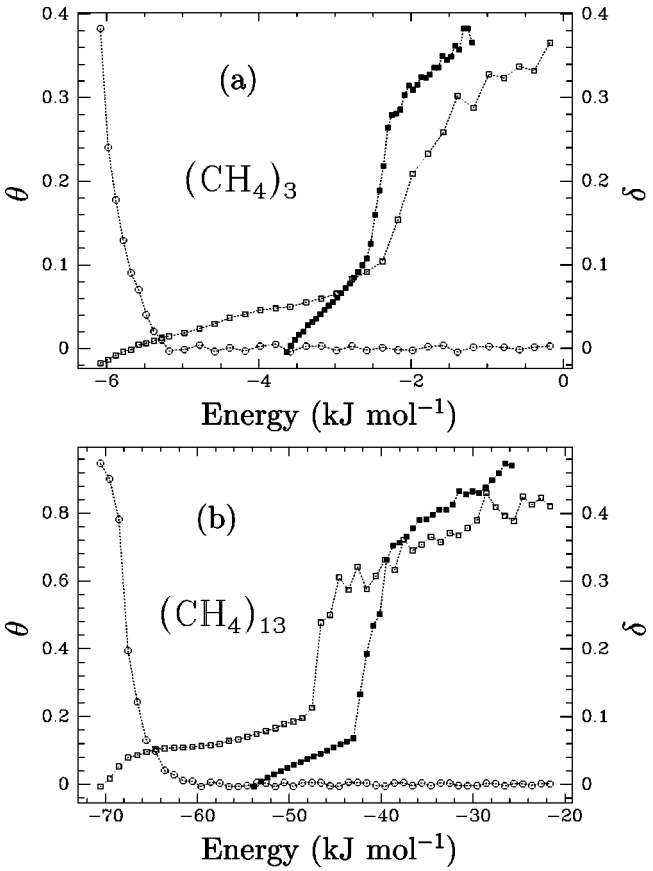

FIG. 1. Translational order parameter (δ, squares) and orientational order parameter (θ, circles) vs total energy E in molecular-dynamics simulations of $(CH_4)_n$ clusters. Values in the all-atom model are represented by empty symbols; values in the united-atom model are represented by full symbols. E is in kJ mol^{-1}, δ and θ have no unit. (a) $n = 3$; (b) $n = 13$.

change appears as a wide peak in the heat capacities, both for $(CH_4)_3$ and $(CH_4)_{13}$ in the UA and AA curves. The absolute difference between the curves is not significant, as it simply results from the larger number of DOF in the AA model. Considering that their parameters were fitted to reproduce bulk properties, the agreement found between these two models is surprisingly good at such small sizes. The link between the phase transitions seen in Fig. 1 and the thermal behavior of Fig. 2 can be realized with the internal energy $U(T)$ plotted in Fig. 3 for both models and sizes. The microcanonical kinetic temperature $T(E)$, not plotted here, remains monotonic whatever the model, and does not show any particular feature such as van der Waals loops characteristic of dynamical coexistence [43].

The melting transition is seen in the microcanonical curves $\delta(E)$ as the sharp jump of δ. For the AA model, this occurs at $E \sim -2$ kj mol^{-1} for $(CH_4)_3$, and $E \sim -47$ kj mol^{-1} for $(CH_4)_{13}$. For the UA model, these values are slightly different, and the rise in δ occurs at $E \sim -2.5$ kj mol^{-1} for $(CH_4)_3$ and $E \sim -40$ kj mol^{-1} for $(CH_4)_{13}$. These values are seen in Fig. 3 to correspond precisely to the melting temperatures at which the heat capacities reach their maximum.

As is apparent from Fig. 1, methane clusters also undergo a transition from orientational order ($\theta \sim 1$) to plasticlike

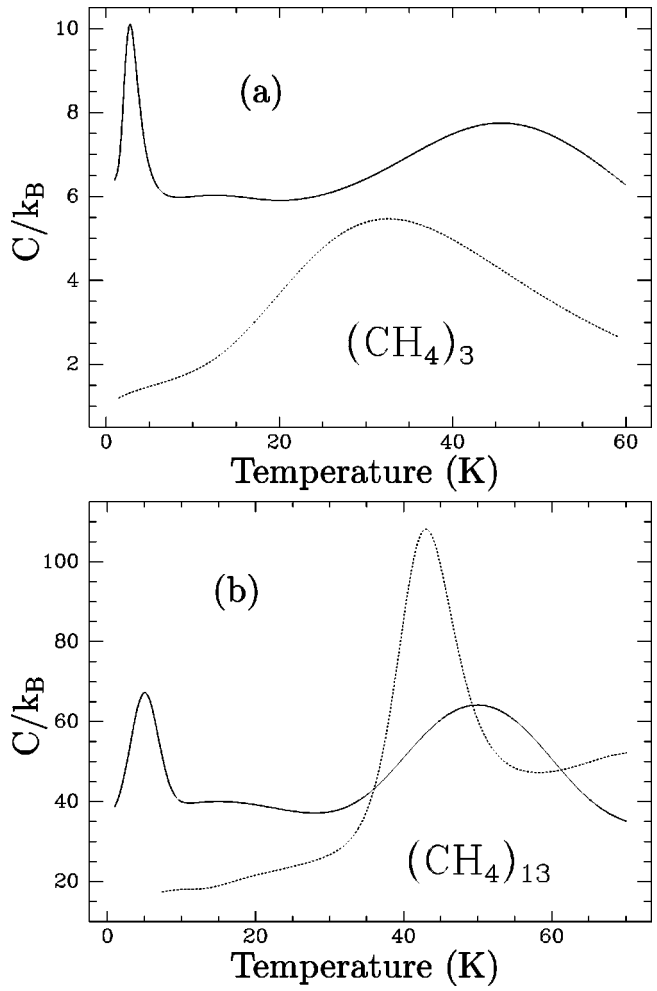

FIG. 2. Configurational heat capacities C vs canonical temperature T for the $(CH_4)_n$ clusters, for the all-atom model (full lines), and for the united-atom model (dashed lines), from molecular-dynamics simulations and the histograms method. C is in units of k_B (Boltzmann's constant), T is in K. (a) $n=3$; (b) $n=13$.

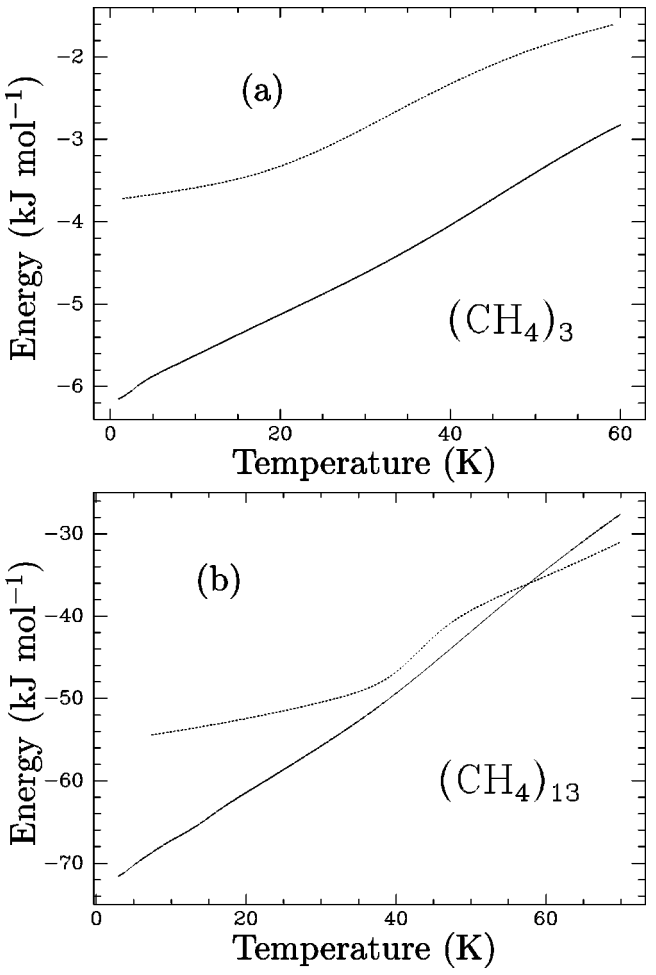

FIG. 3. Internal energy U vs canonical temperature T for the $(CH_4)_n$ clusters, for the all-atom model (full lines), and for the united-atom model (dashed lines), from molecular-dynamics simulations and the histograms method. U is in kJ mol^{-1}, T is in K. (a) $n=3$; (b) $n=13$.

($\theta \sim 0$) at low energy. This transition happens at a much lower energy for $(CH_4)_3$ than for $(CH_4)_{13}$, since θ never reaches values greater than 0.5 for the smaller cluster. From Fig. 3, we interpret the first, narrow peak in the heat capacity (for the AA model) as the thermodynamical consequence of this transition. Similar observations were previously made in numerical experiments on other molecular clusters [44]. Of course, the UA model cannot exhibit any evidence of these rotational effects.

We now come to the maximal Lyapunov exponent λ, plotted in Fig. 4, as well as its translational restriction λ_T for both methane clusters using the two models. Strong similarities are indeed observed between the present curves in the AA model and the results for molecular nitrogen clusters [11]. λ sharply rises as soon as the orientational degrees of freedom are released, while it shows no particular variation when δ jumps above 15%. The variations of λ for the UA model and λ_T for the AA model are much softer. Only λ, in the case of $(CH_4)_3$ for the UA model, shows a clear signature of melting with a drop near $E \sim -2.5$ kJ mol^{-1}. Concerning $(CH_4)_{13}$, both λ and λ_T continuously increase at melting, even if their slopes decrease. Their behaviors at low energy are also very similar, with a rather linear increase just above the binding energy.

It is quite interesting to note that λ_T and λ for the UA model display rather similar behaviors. Of course, due to the much larger number of DOF in the AA model [29], no decrease in λ_T could be reasonably expected for $(CH_4)_3$, while λ drops in the three-atom cluster. However, up to the melting energy, the curves are nearly identical apart from a multiplicative constant. It thus appears that the orientational disorder induces an ''averaging'' effect on the instantaneous intermolecular forces, similar to that in $(N_2)_n$ clusters. This seems to hold as long as the orientational dynamics occur on a much faster time scale than the translational dynamics.

Contrary to the all-atom model, the UA model displays very different behaviors of the largest Lyapunov exponent with total energy. The special case of the trimer has been explained in detail by Wales and Berry [29], who interpreted the drop in λ past isomerization as the result of an increasing harmonicity of the motion near the flat, linear saddle point. No such effect is seen for LJ systems with four atoms or more, but only smooth, monotonic variations. Although this subject is still controversial, it seems that a minimal size of about 40 atoms is required to induce a jump of λ at melting

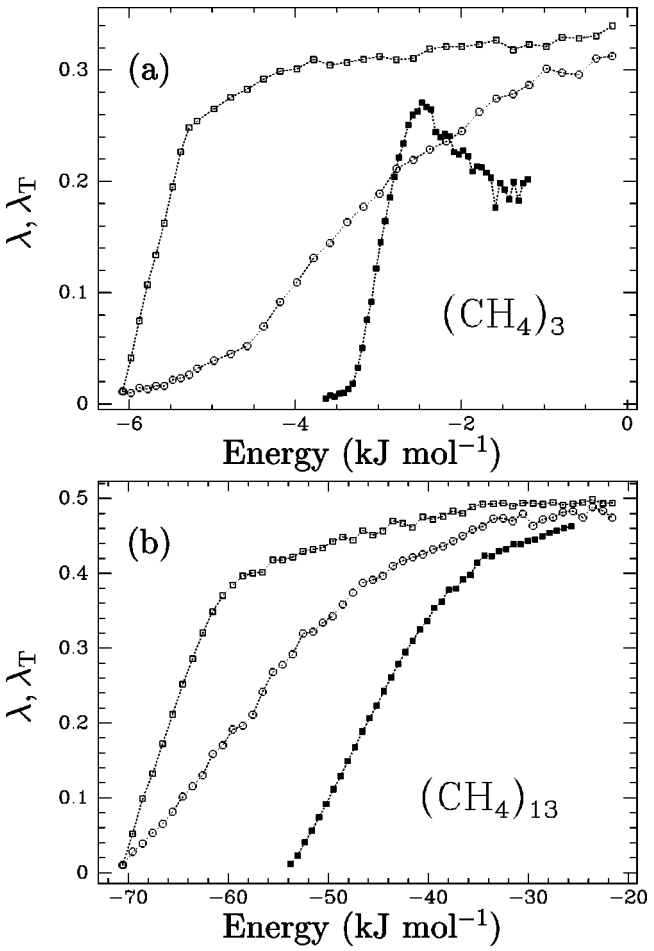

FIG. 4. Largest Lyapunov exponent λ (squares) and translational exponent λ_T (circles) from molecular-dynamics simulations of $(CH_4)_n$ clusters. Values for the all-atom model are represented by empty symbols; values for the united-atom model are represented by full symbols. E is in kJ mol^{-1}, λ and λ_T have no unit. (a) $n=3$; (b) $n=13$.

[31]. In finite systems, this jump is continuous due to dynamical coexistence [31]. A sharp, discontinuous increase should nevertheless occur at bulk limit [10]. In the case of molecular clusters described by all-atom models, no jump in λ is seen at melting. This is not necessarily significant at small size, and a strong increase might appear in periodic systems. However, this surely demands further calculations, for methane as well as for other molecules.

As we have seen, $(CH_4)_n$ clusters share many properties with $(N_2)_n$ clusters. Their thermodynamical behavior involves two phase changes, the first one at low temperatures from an orientationally ordered state to a plastic type phase in which the molecular centers of mass remain in the same geometry while the internal degrees of freedom are released. At higher energies or temperatures, the clusters undergo a more traditional solidlike to liquidlike phase transition with the release of the translational order. Such phenomena are not general to all van der Waals molecular clusters. For instance, $(CO_2)_n$ [44] and $(SF_6)_n$ [45] clusters do not display the solidlike to plasticlike transition in such a distinct way. Carbon dioxide clusters lose their orientational and translational rigidities at the same temperature. On the contrary, sulfur hexafluoride clusters have no (or a very small) orientational rigidity.

As it may be the case for atomic clusters [31], there is not a direct relationship between the possible phase transitions and sudden changes in the largest Lyapunov exponent λ. Nevertheless, and even if the internal degrees of freedom do not necessarily play an important role in the thermal properties of methane clusters once they have been released, they seem to be mainly responsible for the existence of chaos. The nonlinear dynamics of these clusters is indeed very dependent on the potential used to model molecular interactions. This confirms the results of Ohmine and co-workers [12] on the importance of molecular motion on the instantaneous dynamics, as well as recent results on diatomic molecular systems [19,20]. Again, it suggests that one should look at other parameters carrying more information, such as the Kolmogorov entropy, the full Lyapunov spectrum, or the rotation numbers, in order to determine the various contributions to instabilities of all the degrees of freedom.

IV. CONCLUSION

In this paper, we have developed a simple scheme for calculating the Lyapunov characteristic exponents in molecular systems. The method relies on the quaternion formalism of Evans [21], and is not restricted to three-dimensional molecules, even if one can also treat the special case of linear molecules using the method described in the previous paper [11]. In our current approach, the Jacobian matrix between the phase space and the tangent space does not need to be explicitly calculated, and a first-order Taylor expansion of the derivatives (forces, torques, ...) suffices to compute the largest Lyapunov exponent. By considering a basis of $k < 13n$ orthogonal vectors $\delta\psi_i$, the k largest Lyapunov exponents can be estimated by following the time evolution of $\delta\psi_i$ and reorthonormalizing the set $\{\delta\psi_i\}$ regularly. The whole Lyapunov spectrum, in particular, should show $14+2n$ zero exponents [46] due to the conservation of mechanical quantities (14 zeros) and to the quaternion normalization ($2n$ zeros). The method can be employed along with any standard numerical integrator for the propagation of the molecular-dynamics trajectory. It requires the computation of the Hessian matrix of the potential-energy function, and can be applied either to finite or periodic systems. Extension to constant-temperature molecular dynamics is also possible.

We have illustrated this method by investigating the thermodynamics of small $(CH_4)_n$ clusters with $n=3$ and $n=13$ molecules. The influence of the molecular character on the nonlinear dynamics of these clusters was studied with two model potentials: a united-atom potential which considers all the molecules as pseudoatoms interacting through a LJ potential, and an all-atom potential which treats separately carbon and hydrogen atoms with LJ and Coulombic forces. We have shown that the solidlike to liquidlike phase change (near 40 K) follows a rigid to plastic transition occurring at low temperature (near 5 K). This phenomenon has a clear thermal signature, and is responsible for the sharp rise in the largest Lyapunov exponent, at low energies, in the AA model. While the simple UA model cannot display such features, it is still able to reproduce the main trends of the melting process. As is the case for nitrogen clusters [11], chaos in these systems is primarily driven by the internal degrees of freedom, and the loss of translational order does not seem to

induce significant variations in the exponent λ.

The present results emphasize the strong influence of the rotational coordinates on the chaotic dynamics of finite-size clusters. More generally, they also suggest the possible role of parameters such as the Lyapunov exponents of the Kolmogorov entropy to investigate phase transitions and critical phenomena in complex molecular systems.

ACKNOWLEDGMENTS

The author wishes to thank Professor A. H. Fuchs for helpful discussions and Dr. E. Sokell for reading the manuscript. This work was supported by the CNRS, the Région Midi-Pyrénées, the Université Paul Sabatier, and the MENESR.

APPENDIX: IMPLEMENTATION

Solving numerically Eqs. (2)–(5) and (9) together requires two different integrators. For the main trajectory governed by Eqs. (2)–(5), we have chosen the simple leap-frog method of Fincham [24]. This method provides the time evolution of the molecular coordinates $\{\mathbf{r}_i, \mathbf{q}_i\}$ at successive time steps $t_k = k\delta t$, as well as the time evolution of the momenta $\{\mathbf{p}_i, \boldsymbol{\pi}_i\}$ between $t_{k-1/2}$ and $t_{k+1/2}$. We assume that the forces $\{\mathbf{f}_i\}$ and torques $\{\boldsymbol{\tau}_i\}$ are calculated at each time step t_k. To compute the largest Lyapunov exponent with Eq. (9), one first needs to construct an initial $13n$-vector $\delta\psi(0)$, with fixed length, such that $\delta|\mathbf{q}_i|^2 = 0$ for all i. $\delta\psi(t)$ is calculated with, for instance, a Runge-Kutta procedure, by estimating the derivatives in the following simple way.

First of all, Eq. (2) is straightforwardly differentiated as $\delta\dot{\mathbf{r}}_i = \delta\mathbf{p}_i / m_i$. This leads to the explicit form of the matrix $\mathbf{A}$, namely $\mathbf{A} = \mathrm{diag}[1/m_1, 1/m_1, 1/m_1, \ldots, 1/m_n, 1/m_n, 1/m_n]$.

From $\delta\psi(t_k)$, we know the variations $\delta\mathbf{r}_i$ and $\delta\mathbf{q}_i$ for all the molecules. Using Eq. (1), the variations in the quaternions $\delta\mathbf{q}_i$ lead to variations in the rotation matrices $\delta\mathbf{Q}_i$, and hence to variations in the atomic positions. If the molecular interactions are described by site-site interactions, and if s_i denotes the number of interaction sites of molecule i and $\mathbf{d}_i^\alpha$, $1 \leqslant \alpha \leqslant s_i$ the position of site α in the space-fixed reference frame, the variation of the position in the molecule-fixed frame can be written as

$$\delta\mathbf{r}_i^\alpha = \delta[\mathbf{r}_i + \mathbf{Q}_i \cdot \mathbf{d}_i^\alpha] = \delta\mathbf{r}_i + \delta\mathbf{Q}_i \cdot \mathbf{d}_i^\alpha . \tag{A1}$$

The variations of the forces and torques $\delta\mathbf{f}_i$, $\delta\boldsymbol{\tau}_i$ at time t_k may then be calculated using the Hessian matrices of the potential-energy function. This provides the derivatives of the quantities $\delta\mathbf{p}_i$ and $\delta\boldsymbol{\pi}_i$, thus, implicitly, the matrices $\mathbf{D}$, $\mathbf{E}$, $\mathbf{F}$, and $\mathbf{G}$. It remains to estimate the derivatives of $\delta\mathbf{q}_i$. For this, we develop Eq. (5) linearly:

$$\delta\dot{\mathbf{q}}_i = \frac{1}{2}\mathcal{M}(\mathbf{q}_i)\begin{pmatrix} 0 \\ \delta\boldsymbol{\omega}_i^b \end{pmatrix} + \frac{1}{2}\delta\mathcal{M}\begin{pmatrix} 0 \\ \boldsymbol{\omega}_i^b \end{pmatrix}. \tag{A2}$$

$\delta\mathcal{M}$ is directly computed from the expression for $\mathcal{M}$, Eq. (6), and $\delta\boldsymbol{\omega}_i^b$ is easily calculated as a function of $\delta\mathbf{Q}_i$ and $\delta\boldsymbol{\pi}_i$ as

$$\delta\boldsymbol{\omega}_i^b = \mathbf{J}_i^{-1}[\delta\mathbf{Q}_i \cdot \boldsymbol{\pi}_i + \mathbf{Q}_i \cdot \delta\boldsymbol{\pi}_i] \tag{A3}$$

thus providing implicitly the matrices $\mathbf{B}$ and $\mathbf{C}$ of the Jacobian. The use of a leap-frog algorithm for the main MD trajectory also implies a further evaluation, at each time step t_k, of the values of the angular momenta $\{\boldsymbol{\pi}_i\}$ from their values at $t_{k-1/2}$. In practice, this is already done in the method of Fincham [24].

[1] J.-P. Hansen and I. R. McDonald, *Theory of Simple Liquids*, 2nd ed. (Academic Press, New York, 1986).
[2] B. L. Holian, W. G. Hoover, and H. A. Posch, Phys. Rev. Lett. **59**, 10 (1987).
[3] H. A. Posch and W. G. Hoover, Phys. Rev. A **38**, 473 (1988); **39**, 2175 (1989).
[4] H. A. Posch, W. G. Hoover, and B. L. Holian, Ber. Bunsenges. Phys. Chem. **94**, 250 (1990).
[5] P. Butera and G. Caravati, Phys. Rev. A **36**, 962 (1987); A. Bonasera, V. Latora, and A. Rapisarda, Phys. Rev. Lett. **75**, 3434 (1995).
[6] F. Calvo and P. Labastie, J. Phys. Chem. B **102**, 2051 (1998).
[7] L. Casetti, R. Livi, and M. Pettini, Phys. Rev. Lett. **74**, 375 (1995); L. Casetti, C. Clementi, and M. Pettini, Phys. Rev. E **54**, 5969 (1996).
[8] V. Mehra and R. Ramaswamy, Phys. Rev. E **53**, 3420 (1996).
[9] Y. S. Fan and T. R. Chay, Phys. Rev. E **51**, 1012 (1995).
[10] K.-H. Kwon and B.-Y. Park, J. Chem. Phys. **107**, 5171 (1997); S. K. Nayak, P. Jena, K. D. Ball, and R. S. Berry, *ibid.* **108**, 234 (1998).
[11] F. Calvo, Phys. Rev. E **58**, 5643 (1998).
[12] M. Cho, G. R. Fleming, S. Saito, I. Ohmine, and R. M. Stratt, J. Chem. Phys. **100**, 6672 (1994); S. Saito and I. Ohmine, *ibid.* **108**, 240 (1998).
[13] S. Saito and I. Ohmine, J. Chem. Phys. **102**, 3566 (1995); **106**, 3329 (1997).
[14] M. Buchner, B. M. Ladanyi, and R. M. Stratt, J. Chem. Phys. **97**, 8522 (1992).
[15] J.-B. Maillet, A. Boutin, S. Buttefey, F. Calvo, and A. H. Fuchs, J. Chem. Phys. **109**, 329 (1998).
[16] C. Amitrano and R. S. Berry, Phys. Rev. Lett. **68**, 729 (1992).
[17] C. Seko and K. Takatsuka, J. Chem. Phys. **104**, 8613 (1996); M. A. Miller and D. J. Wales, *ibid.* **107**, 8568 (1997).
[18] C. Dellago and H. A. Posch, Phys. Rev. E **52**, 2401 (1995); C. Dellago, L. Glatz, and H. A. Posch, *ibid.* **52**, 4817 (1995); C. Dellago, H. A. Posch, and W. G. Hoover, *ibid.* **53**, 1485 (1996).
[19] I. Borzsák, H. A. Posch, and A. Baranyai, Phys. Rev. E **53**, 3694 (1996).
[20] O. Kum, Y. H. Shin, and E. K. Lee, Phys. Rev. E **58**, 7243 (1998).
[21] D. J. Evans, Mol. Phys. **34**, 317 (1977).
[22] H. Goldstein, *Classical Mechanics*, 2nd ed. (Addison-Wesley, Reading, MA, 1980).

[23] M. P. Allen and D. J. Tildesley, *Computer Simulations of Liquids* (Oxford University Press, Oxford, 1987).
[24] D. Fincham, Daresbury Laboratory Quarterly for MD and MC Simulations, Report No. 2 (1981), p. 6.
[25] G. Benettin, L. Galgani, and J.-M. Strelcyn, Phys. Rev. A **14**, 2338 (1974).
[26] F. Calvo and E. Yurtsever (unpublished).
[27] W. G. Hoover and H. A. Posch, Phys. Lett. **113A**, 82 (1985); W. E. Wiesel, Phys. Rev. E **47**, 3686 (1993).
[28] T. L. Beck, D. M. Leitner, and R. S. Berry, J. Chem. Phys. **89**, 1681 (1988); R. J. Hinde, R. S. Berry, and D. J. Wales, *ibid.* **96**, 1376 (1992); C. Amitrano and R. S. Berry, Phys. Rev. E **47**, 3158 (1993); S. K. Nayak, R. Ramaswamy, and C. Chakravarty, *ibid.* **51**, 3376 (1995).
[29] D. J. Wales and R. S. Berry, J. Phys. B **24**, L351 (1991); R. J. Hinde and R. S. Berry, J. Chem. Phys. **99**, 2942 (1993).
[30] V. Mehra and R. Ramaswamy, Phys. Rev. E **56**, 2508 (1997).
[31] F. Calvo, J. Chem. Phys. **108**, 6861 (1998).
[32] G. Torchet, J. Farges, M.-F. De Feraudy, and B. Raoult, in *Proceedings of the International School of Physics Enrico Fermo, Course VII*, edited by G. Scoles (North-Holland, Amsterdam, 1990), p. 513.
[33] A. Vishnyakov, E. M. Piotrovskaya, and E. N. Brodskaya, J. Chem. Phys. **106**, 1593 (1997).
[34] W. L. Jorgensen, M. D. Madura, and C. J. Swenson, J. Am. Chem. Soc. **106**, 6638 (1984).
[35] B. Chen, M. G. Martin, and J. I. Siepmann, J. Phys. Chem. B **102**, 2578 (1998).
[36] W. L. Jorgensen, D. S. Maxwell, and J. Tirado-Rives, J. Am. Chem. Soc. **118**, 11 225 (1996).
[37] D. J. Wales and J. P. K. Doye, J. Phys. Chem. A **101**, 5111 (1997).
[38] D. J. Wales and M. P. Hodges, Chem. Phys. Lett. **286**, 65 (1998).
[39] S. Xu and L. S. Bartell, J. Phys. Chem. **97**, 13 544 (1993).
[40] R. A. Radev, A. Proykova, F.-Y. Li, and R. S. Berry, J. Chem. Phys. **109**, 3596 (1998).
[41] A. H. Fuchs and G. S. Pawley, J. Phys. (Paris) **49**, 41 (1988).
[42] F. Calvo and P. Labastie, Chem. Phys. Lett. **247**, 395 (1995).
[43] D. J. Wales, Mol. Phys. **78**, 151 (1993).
[44] J.-B. Maillet, A. Boutin, and A. H. Fuchs, Phys. Rev. Lett. **76**, 4336 (1996).
[45] A. Boutin, J.-B. Maillet, and A. H. Fuchs, J. Chem. Phys. **99**, 9944 (1993).
[46] H. D. Meyer, J. Chem. Phys. **84**, 3147 (1986).